Proceedings of Engineering & Technology -PET Vol 96, pp.46-53 **Advances in Energy Transition and Environmental Impacts**

Characterization of a super hydrophobic soot-coated glass insulator

N. Rouha[#1], N. Bouzidi[#2], A. Beroual[#3]

[#1] *Laboratoire de Génie Electrique, Faculté de Technologie, Université de Bejaia, 06000, Algérie*
[1]nacera.rouha@univ-bejaia.dz

[#2] *Laboratoire de Génie des Procédés, Faculté de Technologie, Université de Bejaia, 06000, Algérie*
[2]nedjima.bouzidi@univ-bejaia.dz

[#3] *Ecole Centrale de Lyon - AMPERE Lab UMR CNRS 5005, 36 Avenue Guy de Collongue, 69130 Ecully, France*
[3]Abderrahmane.beroual@ec-lyon.fr

***Abstract*— Deal with electrical flashovers problems, insulating materials with superhydrophobic surface are ideal for manufacturing insulator systems to improve their performances. This paper deals with the electrical aging phenomenon effect on the hydrophilic and superhydrophobic surface of glass insulators in service. At this purpose, a physicochemical experimental study of glass (G) and soot-coated glass (SCG) insulators electrically aged under wet conductive pollution is undertaken. At first, accelerated electrical degradation tests were conducted under a growing alternating 50 Hz homogeneous electrical field on glass and soot-coated glass samples. A series of surfacic breakdown is carried out on these two materials in both clean and polluted surfaces to characterize their performances. The measurements of the contact angle, the dielectric strength, the capacitor and the loss factor are performed on virgin (Vg) and electrically aged (EA) samples in the two surface states; clean (C) and polluted (P). This latter case is performed using wet conductive pollutant with electrical conductivity of 2 mS/cm^2 and 5 mS/cm^2. Then series of chemical analyses, as a light microscopy (LM) analysis, an Infrared spectroscopy FTIR and X-ray diffraction analysis (XRD) were performed to monitor the degradation at microscopic scale. Electrical and chemical measurements have evidenced the constraints effects on the G and SCG aging phenomenon, and a correlation between the different results was established.**

***Keywords*— Aging, light microscopy, Infrared spectroscopy, X-ray diffraction analysis, Pollution, Soot-coated glass.**

I. INTRODUCTION

Flashover phenomena compromise electrical energy transmission and high-voltage infrastructure durability [1], [2]. Natural and industrial contaminants aggravate this issue, particularly under elevated humidity conditions [3]-[6]. This is because humidification of the pollution layer triggers insulator flashover, disrupting transmission networks. Indeed, when subjected to an electric field, a water droplet accumulated on the external insulator surface can deform, generating an intense localized field that disrupts the surrounding environment. This can trigger partial discharges, which may escalate into an electric arc, ultimately leading to insulator flashover [7], [8]. Utilizing hydrophobic and superhydrophobic materials offers a viable solution to this issue, as they effectively reduce leakage currents and decrease the likelihood of dry band formation, thereby enhancing insulation performance in polluted environments [9]-[12].

This study focuses on the physicochemical analysis of electrically aged glass (G) and soot-coated glass (SCG) insulators. It aims to assess the contact angle (θ), dielectric strength (E_l), capacitance (C_x), and loss factor ($tg\delta$) before and after aging, both with and without pollution effects. The material's behavior at the molecular level is examined through chemical analyses, including Light Microscopy LM analysis, FTIR infrared spectroscopy and XRD X-ray diffraction, to characterize the impact of electrical degradation under polluted conditions on its microstructure.

II. EXPERIMENT

The investigations are carried out on parallelepiped G and SCG film samples 100 × 100 × 5 mm^3 in dimensions. The accelerated electrical degradation tests are performed under increasing uniform field, under AC - 50 Hz voltage ramp with speed of 2kV$_{max}$/s. A series of 100 surface flashover is carried out with a plane-plane electrode geometry (fig.1). Polluted (P) and clean (C) G and SCG surface conditions are considered. The pollutant used is a sodium chloride solution (NaCl) with two electrical conductivities namely, σ = 5 mS/cm^2 and σ = 2 mS/cm^2, noted (2) and (5) respectively. Series of physical and electrical measurements and chemical analyses are conducted on virgin in clean surface (VgC), virgin in polluted surface (VgP), electrically aged in clean surface (EAC) and electrically aged in polluted surface (EAP) conditions G and SCG samples. Contact angle *(θ)*, longitudinal dielectric strength (E_l), capacitance (C_x) and loss factor ($tg\delta$)

ISSN: 1737-9334

Proceedings of Engineering & Technology -PET Vol 96, pp.46-53 **Advances in Energy Transition and Environmental Impacts**

measurements are undertaken. θ is determined in the horizontal plane of the glass plate surface, for a droplet volume V=4µl (fig. 2). C_x and $tg\delta$ are measured under a voltage levels V_{rms} = 100 V at increasing frequencies (f = 100 Hz to 1100 Hz in increasing steps from 10 to 100 Hz) using Schering bridge. To monitor the degradation at microscopic scale, the following analyses are conducted: LM is performed with a magnification of 400 and 1000. It allows to relevantly seeing the changes occurred on the relief material. FTIR is carried out by subjecting the samples to electromagnetic radiation in the infrared wavelength range of 2.5 µm <λ <50 µm. Samples are exposed to XRD with a wavelength beam (0.1 nm < λ < 10 nm).

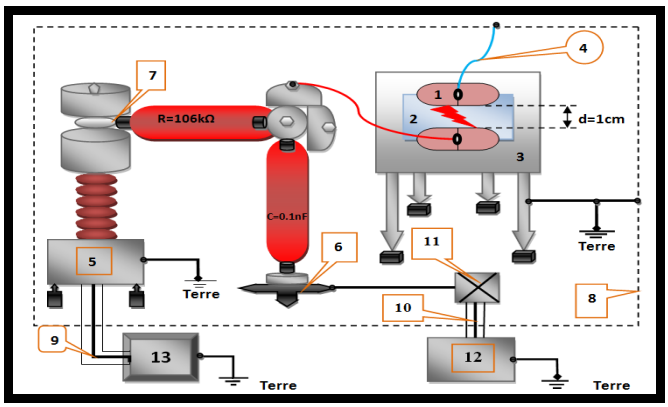

Fig. 1 Experimental device of electrical aging

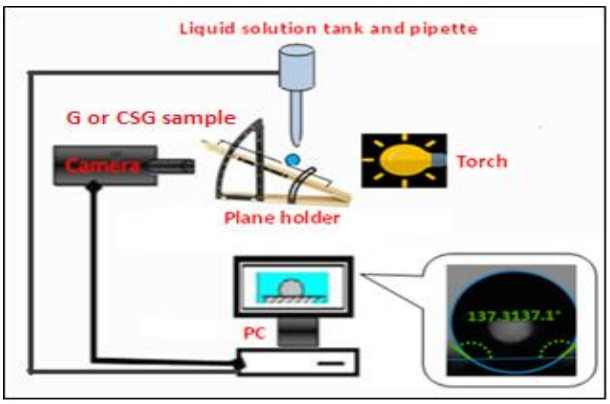

Fig. 2 Experimental setup of contact angle θ measurement

Where, 1: Copper electrode, 2: Solid materials (G or CSG), 3: Table. 4: Wire, 5: High voltage transformer, 6: Element support, 7: Connection nodes, 8: Protection grid, 9 and 10: Coaxial cable, 11: Connection box, 12: MU11 Peak Voltmeter, 13: SG1BT manual and automatic control system.

III. EXPERIMENTAL RESULTS

A. Aging and Pollution Effects on G and SCG Electrical Performance

The electrical aging affects both G and SCG longitudinal dielectric strength (Table I). This quantity decreases under the effect of electrical stress. The soot coating increases the surface conductivity of the glass, further degrading its dielectric strength. In the presence of conductive pollution deposits, this reduction worsens. And it is even more marked when the conductivity of the polluting layer is increased (Fig. 3). The work of the authors [13] and [14] has a slight approach with those presented above relating to the G insulator. G and SCG electrical aging leads to a reduction of Cx, which decreases more significantly with higher voltage frequency (Fig. 4). The decline in this value indicates material deterioration, which is more significant in the presence of pollution. A slight approach to G results can be made with those of [15]. The G loss factor $tg\delta$ decreases as the frequency of the excitation (or measurement) signal increases. This result implies that the material responds in frequency like an equivalent circuit with localized parallel RC constants, making it well-suited for high-frequency operation due to its superior energy quality efficiency. The electrical aging leads to an increase in the loss factor, which becomes more pronounced with the rise in conductivity of the polluted layer. $Tg\delta$ is more important in the EAP case compared to the EAC and Vg one (Fig. 5). A slight approach to G results can be made with those of [15].

ISSN: 1737-9334

TABLE I

LONGITUDINAL DIELECTRIC STRENGTH EL

Longitudinal dielectric strength El (kV/cm)						
State		VgC	VgP wet pollution σ=2 mS/cm^2	VgP wet pollution σ=5 mS/cm^2	EAC	EAP wet pollution σ=2 mS/cm^2	EAP wet pollution σ=5 mS/cm^2
G	a	15.26					
	b				14.04		
	c		12.86				
	d			11.58			
	e					10.54	
	f						8.4
SCG	g	13.2					
	h				12.12		
	i		11.34				
	j			9.5			
	k					9.40	
	l						7.36

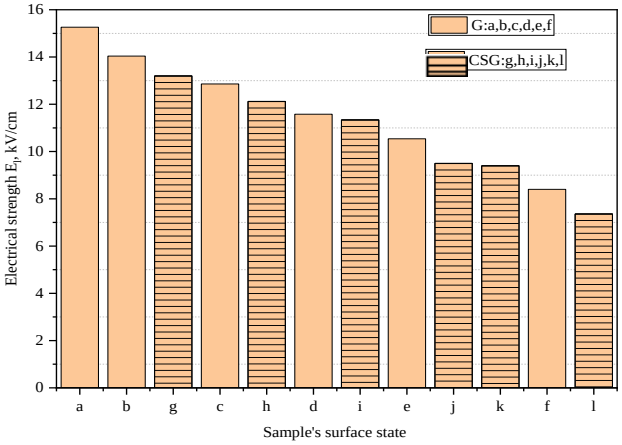

Fig. 3 El Histogram versus G and SCG surface condition

Where: for G (a: VgC, b: EAC, c: VgP at σ=2 mS/cm^2, d: VgP at σ=5 mS/cm^2, e: EAP at σ=2 mS/cm^2 and f: EAP at σ=5 mS/cm^2), and for SCG (g: VgC, h: EAC, i: VgP at σ=2 mS/cm^2, j: VgP at σ= 5 mS/cm^2, k: EAP at σ=2 mS/cm^2 and ℓ: EAP at σ=5 mS/cm^2).

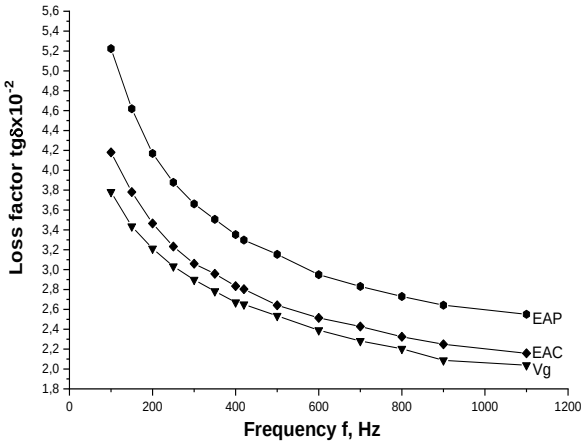

Fig. 4 Cx versus frequency for different G states: virgin, aged in clean and polluted conditions

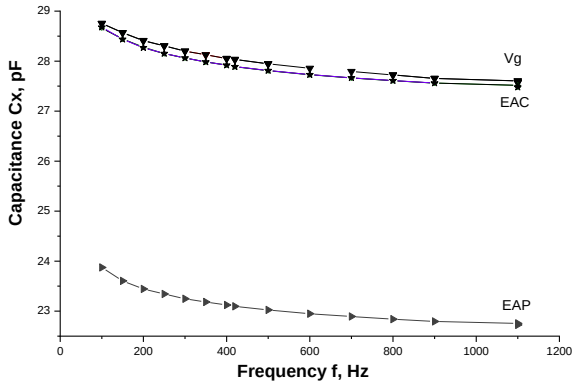

Fig. 5 tg δ versus frequency depending on G states: virgin, aged in clean and polluted conditions

B. Aging and Pollution Effects on G and SCG hydrophilic and superhydrophobic Performance

In its youthful state (VgC), G is hydrophilic (figs. 6 and 7.A) [16]. Its aging (EAC) caused by multiple flashover and imposed pollution conditions (EAP2 and EAP5) at σ=2mS/cm^2 and σ=5mS/cm^2 respectively, leads to an attenuation of this characteristic, which is however less pronounced in the case of severe pollution, which damages its surface without making it hydrophobic (fig. 6). Conversely, SCG is superhydrophobic in its youth (VgC) (figs. 6 and 7.B), and its aging partially affects this characteristic (EAC), especially in the presence of wet pollution (EAP). This last point agrees with the results of [16] carried out on G insulator. However, severe pollution intensifies the discharge which sweeps away soot in its path, and the dust cloud formed strengthens its peaks, which compensates for this loss and allows the material to regain its superhydrophobic characteristic (fig. 6).

ISSN: 1737-9334

Proceedings of Engineering & Technology -PET Vol 96, pp.46-53 **Advances in Energy Transition and Environmental Impacts**

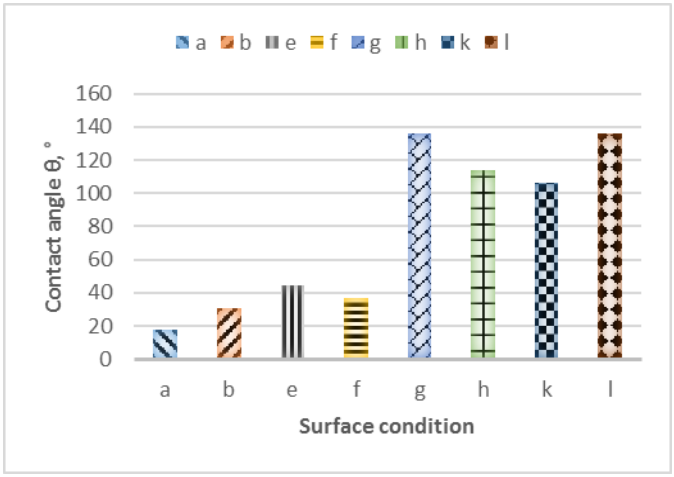

Fig. 6 θ Histogram versus G and SCG surface condition

A  B  C

Fig. 7 Water droplet on: A) hydrophilic G and B) and C) superhydrophobic SCG surface

C. Aging and Pollution Effects on G and SCG Surface Morphology

The observations and photographic shoot made with LM analysis of G and SCG samples aged under electric field stress in the clean and polluted state revealed traces left by the discharge. The latter caused a carbonization and a surface depolishing of G sample, which becomes rough, giving it a quasi-hydrophobic character (fig. 6, 8.B and 8.C), unlike the superhydrophobic character of the SCG sample, which is affected. However, its aging under severe pollution at $\sigma = 5$ mS/cm^2 promotes the electrical arcing initiation following the establishment of a leakage current through the superficial layer; This reveals, over the entire surface, sinuous traces of the tree-like discharge that sweeps away soot in its path, thus promoting the formation of peaks. This gives the surface a rough appearance which improves its superhydrophobic character (fig. 6, 7.B and 8.D).

ISSN: 1737-9334

Proceedings of Engineering & Technology -PET Vol 96, pp.46-53 **Advances in Energy Transition and Environmental Impacts**

A. VgC-G (a) sample B. EAC-G (b) sample C. EAP5-G (f) sample D. EAP5-SCG (ℓ) sample

Figure 8. LM photographic of G and SCG samples

D. Aging and Pollution Effects on G and SCG Molecular Structure

FTIR analysis revealed two distinct regions: the first region starting from 4000 to 1500 cm^{-1} related to hydroxyl groups (O-H) and groups linked to bonds (C-H and C-O, C=O, C=C); the second region, ranging from 1600 to 400 cm^{-1}; related to the compound's fingerprint and the different groups characterizing structural bonds generally linked to glass (Si-O, Al-O, etc.) (fig.9). Thus, very broad bands located between 991 and 1021 cm^{-1} are observed; they are attributed to the Si-O bond related to glass. However, pollution caused two broad bands to appear at 3430 and 1670 cm^{-1} for samples e (G-EAP2 and f (G-EAP5); these are attributed to the presence of external hydroxyl groups of O-H characterizing H-O-H bonds.

The application of soot on glass revealed several bands characterizing the bonds of the organic compounds making up the soot; furthermore, the influence of aging and pollution on the soot associated with the glass is revealed by the pronounced presence of new vibration bands.

The spectra of samples g (SCG-VgC), h (SCG-EAC), k (SCG-EAP2) and ℓ (SCG-EAP5) show the presence of peaks characterizing the functional groups at 2962, 2932 and 2859 cm^{-1} for CH2 and CH3 bonds respectively; related to the aliphatic cycles of soot. These peaks are much more intense when the samples are not subjected to pollution (samples g and h). On the other hand, as pollution increases, broad bands appear around 3430 cm^{-1} which are attributed to the presence of external OH indicating the presence of water (H-O-H).

In the spectrum (1600-500 cm^{-1}), several intense bands appear, attributed to the different aromatic cycles making up the soot. The bands noted at 1470 cm^{-1} are attributed to the functional groups of the C-H bonds of the aliphatic cycles CH2 and CH3, these peaks become much more intense as pollution increases.

On the other hand, a broad band at 1650 cm^{-1} is observed, attributed to the presence of aromatic cycles C-C, C-H, and C-O-C. The structure of the glass is greatly influenced by the presence of soot and pollution, which is noted by the presence and broadening of the peaks at 991 cm^{-1}, related to the Si-O bond.

The X-ray spectra recorded in 2θ between 5° and 80° show the almost complete absence of crystalline phases, which indicates that the glasses have a totally amorphous structure, noted by the hump that exists between 20 – 25 [°2Θ]. However, some peaks appear between (27.47 - 36.13 and 54.38) [°2Θ] characteristic of rutile and a crystalline phase of Chromium Manganese Telluride which diffracts at (28.40 and 29.49) [°2Θ]. Note, however, the shift towards small angles of the XRD spectrum of sample h (SCG-EAC) relative to samples a (G-VgC) and b (G-EAC), as well as the disappearance of the hump at angle 12 [°2θ] of sample ℓ (SCG-EAP5) relative to samples f (G-EAP5) and g (SCG-VgC). This suggests that electrical aging and

ISSN: 1737-9334

pollution have effects on the structure of the soot or the soot-glass interaction. The pollutant could have an impact on the charge distribution at the glass surface and modify the interaction between the soot and the glass. The changes in surface morphology observed in ML suggest that the pollutant (NaCl) could modify the soot structure, making it more compact or uniform, create nucleation sites for deposit growth, and influence the mobility of species on the glass surface, which would explain the loss of the hump in the XRD spectrum, as the soot structure is modified.

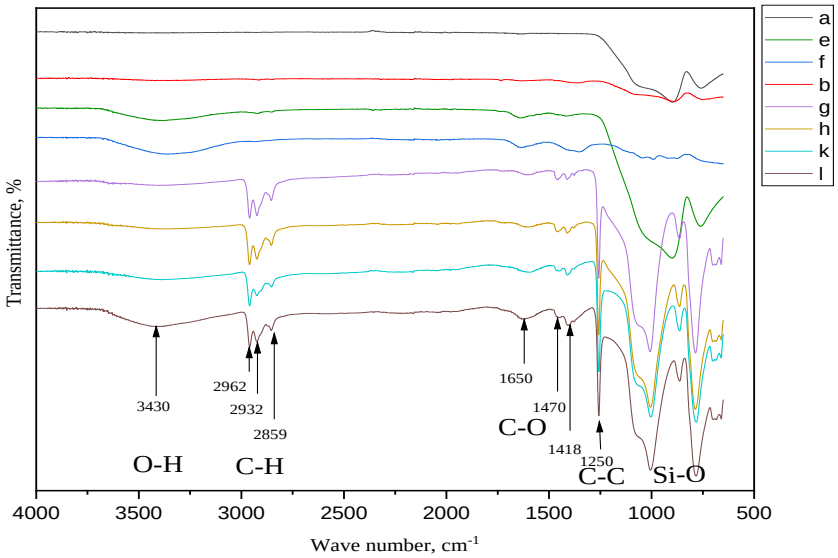

Fig. 9 FTIR spectra of G and SCG samples (virgin and aged, polluted at σ=2mS/cm^2 and at σ=5mS/cm^2)

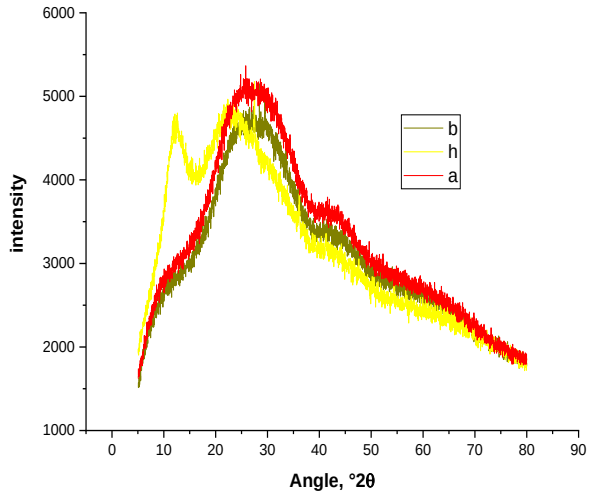

Fig. 10 X-ray diffractogram of different glass samples: a (G-VgC), b (G-EAC) and h (SCG-EAC)

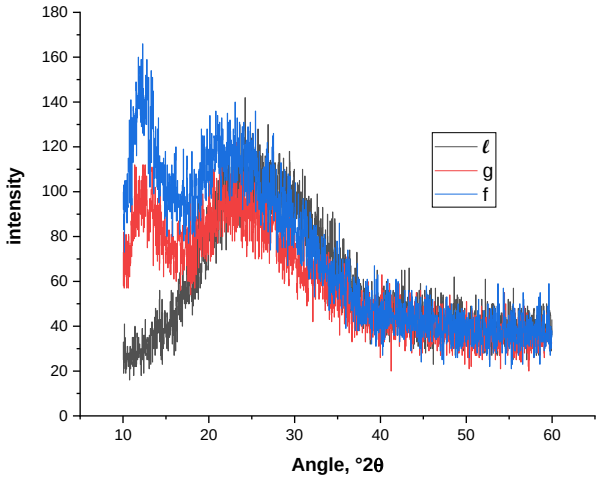

Fig. 11 X-ray diffractogram of different glass samples: f (G-EAP5), g (SCG-VgC) and ℓ (SCG-EAP5)

IV. CONCLUSION

The results of electrical and physical measurements, supported by a light microscopy (LM), X-ray diffraction (XRD) and Infrared spectroscopy (FTIR) analyses, showed that the glass structure is highly influenced by aging and the presence of soot and pollution, and that electrical aging under severe pollution conditions (conductivity σ=5 mS/cm^2) degrades the electrical properties of the glass (dielectric strength E_l, electrical loss factor tgδ, capacitance Cx).

This is revealed by FTIR analyses highlighting the presence of peaks characterizing the functional groups of CH2 and CH3 bonds related to the aliphatic cycles of soot, and the appearance of several intense bands attributed to the various aromatic cycles composing the soot C-C, C-H, and C-O-C, as well as by the

ISSN: 1737-9334

broadening of peaks related to the Si-O bond. Similarly, LM and XRD analyses revealed the electrical aging and pollution effects on the structure of the soot and the soot-glass interaction. XRD lets suggest that the pollutant could have an impact on the charge distribution at the glass surface and modify the interaction between the soot and the glass. Likewise, LM analysis revealed changes in surface morphology related to the NaCl pollutant which could modify the soot structure, making it more compact or uniform, create nucleation sites for deposit growth, and influence the mobility of species on the glass surface.

Thus, the glass degradation under the applied field stress and the presence of soot and pollution can be directly linked to the embrittlement of this material following the phase change, the oxidation mechanism produced, and the alteration of its surface under the effect of intense discharge energy, which results in a decrease in its electrical and physical performance. The polar nature of the conductive pollutant solution (NaCl) contributes to this degradation.

In contrast, the application of electrical field stress, combined with the presence of severe pollution, improves the hydrophobic, or even superhydrophobic, character of its surface by making it rough; this lowers the surface energy and makes the contact area between the solid (glass) and the fluid (droplets) negligible. This can be explained by the nano- and micro-structured arrangement produced by the discharge, and by the large amount of air that is trapped in the topography, which makes the friction between water and air, and air and air almost zero [17].

REFERENCES

[1] R. N. R. Ghaly, A. Ibrahim, S. S. M. Ghoneim, A. Abu-Siada, M. Bajaj, I. Zaitsev and H. Awad, “Impact of atmospheric conditions on the flash-over voltage of the transmission line insulators using central composite design”, Scientific Reports, 2024, 14:22395 https://doi.org/10.1038/s41598-024-72815-z

[2] Gebczyk, K., Chojnacki, A. L., Grakowski, L. & Banasik, K., “ Failures of insulators in low voltage overhead lines”, Progress Appl. Electr. Eng. (PAEE), 2019, https://doi.org/10.1109/PAEE.2019.8789000

[3] M. Latif and Suwarno, "Performance of 20 kV Epoxy Resin Outdoor Insulator Under Various Environment Conditions," 2006 IEEE 8th International Conference on Properties & applications of Dielectric Materials, pp. 353-356, 2006, https://doi.org/10.1109/ICPADM.2006.284188

[4] Salem, A. A. et al., “Pollution Flashover voltage of transmission line insulators: Systematic review of experimental works”, IEEE Access 10, pp. 10416–10444, 2022, https://doi.org/10.1109/ACCESS.2022.3143534

[5] I. Gutman, K. Halsan, J. Seifert, and W. Vosloo, “Pollution & Ageing Per formance of Composite DC Line Insulators: Service & Test Experience”, INMR, Issue 92, Quarter 2, Volume 19, No. 2, pp. 76-81, 2011

[6] D. Pylarinos, K. Siderakis, E. Thalassinakis, “Comparative investigation of silicone rubber composite and room temperature vulcanized coated glass insulators installed in coastal overhead transmission lines”, IEEE Electrical Insulation Magazine, Vol. 31, Issue 2, pp. 23-29, March-April 2015, https://doi.org/10.1109/MEI.2015.7048134

[7] V. Mohan, K. Chandrasekharan, K. Padmanabhan, “Marangoni effects under electric fields”, Adv. Space Res., 3, (5), pp. 177–180, , 1983

[8] S. Deb, R. Ghosh, S. Dutta, S. Dalai and B. Chatterjee, "Effect of humidity on leakage current of a contaminated 11 kV Porcelain Pin Insulator," 6th International Conference on Computer Applications In Electrical Engineering-Recent Advances (CERA), pp. 215-219, 2017, https://doi.org/10.1109/CERA.2017.8343329

[9] J. Ndoumbe, “Etude Comportementale des Gouttes d’Eau Déposées sur la Surface d’un Isolateur Composite Haute Tension en Présence du Champ Electrique“, phD Thesis, Ecole Centrale de Lyon, 2014

[10] J. M. George, S. Prat, C. Lumb, F. Virlogeux, I. Gutman, J. Lundengård, M. Marzinotto, “ Field Experience and Laboratory Investigation of Glass Insulators having a Factory-applied Silicone Rubber Coating”, IEEE Transactions on Dielectrics and Electrical Insulation Vol. 21, No. 6; December 2014, https://doi.org/10.1109/TDEI.2014.004600

[11] Wibowo, Ari. “Increasing the performances of various Types Outdoor Insulators by using RTV Silicone Rubber Coating”, International Journal on Electrical Engineering and Informatics, Vol. 4, pp. 608-619, 2012

[12] F. Pratomosiwi, S. Suwarno, “Performance Improvement of the Ceramic Outdoor Insulators Located at Highly Polluted Environment Using Room Temperature Vulcanized Silicone Rubber Coating”, International Journal on Electrical Engineering and Informatics, Vol. 2, pp.15-28, 2010

[13] T. Su, S. B. Yaakob, and A. M. Ariffen, “Modelling and analysis of electrical performance outdoor glass insulator under various services and lightning impulse,” J. Phys. Conf. Ser., Vol. 2550, 012021, 2023, https://doi.org/10.1088/1742-6596/2550/1/012021

[14] A. A. Salem, R. Abd-Rahman, W. Rahiman, S. A. Al-Gailani, S. M. Al-Ameri, M. T. Ishak, U. U. Sheikh, "Pollution Flashover Under Different Contamination Profiles on High Voltage Insulator: Numerical and Experiment Investigation", IEEE Access, 9, pp. 37800–37812, 2021. https://doi.org/10.1109/ACCESS.2021.3063201

[15] B. Dolnik, “Measurement of dielectric loss factor and capacity on high voltage glass and silicon rubber insulating material”, Mandely Data, sep. 2024, https://doi.org/10.17632/9rwnnt9t9n.1

[16] A. Bagaskara, Rachmawati and Suwarno, “Comparison Study of Insulation Performance of Semiconducting Glaze, Ceramic, and Glass Outdoor Insulators with Artificial Conditions”, International Journal on Electrical Engineering and Informatics - Volume 16, Number 3, September 2024, https://doi.org/10.1109/ICPADM.2006.284188

[17] N. Rouha, T. Belhoul, N. Bouzidi, A. Beroual, “Characterization of a super hydrophobic soot-coated glass insulator subjected to aging and pollution”, The 3rd Electrical Engineering International Conference (EEIC’25), Bejaia, December 02-03, 2025

ISSN: 1737-9334